

# Towards Unsupervised Sketch-based Image Retrieval

Conghui Hu<sup>1</sup> Yongxin Yang<sup>1</sup> Yunpeng Li<sup>1</sup> Timothy M. Hospedales<sup>2</sup> Yi-Zhe Song<sup>1</sup>  
<sup>1</sup>University of Surrey <sup>2</sup>University of Edinburgh

## Abstract

Current supervised sketch-based image retrieval (SBIR) methods achieve excellent performance. However, the cost of data collection and labeling imposes an intractable barrier to practical deployment of real applications. In this paper, we present the first attempt at unsupervised SBIR to remove the labeling cost (category annotations and sketch-photo pairings) that is conventionally needed for training. Existing single-domain unsupervised representation learning methods perform poorly in this application, due to the unique cross-domain (sketch and photo) nature of the problem. We therefore introduce a novel framework that simultaneously performs unsupervised representation learning and sketch-photo domain alignment. Technically this is underpinned by exploiting joint distribution optimal transport (JDOT) to align data from different domains during representation learning, which we extend with trainable cluster prototypes and feature memory banks to further improve scalability and efficacy. Extensive experiments show that our framework achieves excellent performance in the new unsupervised setting, and performs comparably or better than state-of-the-art in the zero-shot setting.

## 1. Introduction

Sketches efficiently convey the shape, pose and fine-grained details of objects, and thus are particularly valuable in serving as queries to conduct retrieval of photos, *i.e.*, sketch-based image retrieval [29, 37] (SBIR). SBIR has been increasingly well studied, leading to continual improvements in retrieval performance [31, 1]. However state-of-the-art methods generally bridge the sketch-photo domain gap through supervised learning using sketch-photo pairs, for example with triplet ranking [37, 29]. This supervised learning paradigm imposes a severe bottleneck on the feasibility of SBIR in practice. In order to achieve effective SBIR for a certain category, expensive sketch-photo pairing and class annotations are required for model training. The main research direction on reducing annotation cost thus far has been zero-shot SBIR [9, 22], where labeled data is no longer necessitated for the few unseen categories, yet the problem still requires availability of all category labels and

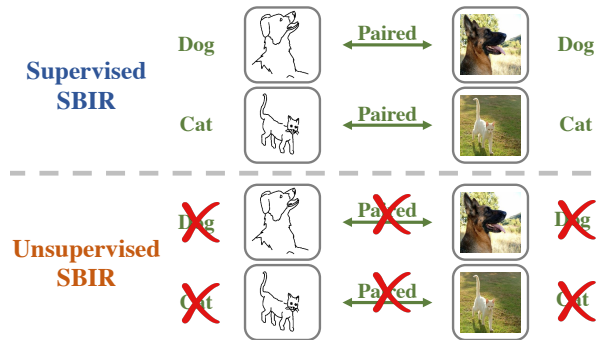


Figure 1. Illustration of unsupervised SBIR where no class label or pairing information is available during training.

specific pairing annotations for the *seen* categories.

In this paper we go to the extreme in addressing the annotation bottleneck, and study for the first time the problem of *unsupervised* SBIR, where we work under the stringent assumption of (i) no sketch-photo pairing, and (ii) no category annotations (as illustrated in Figure 1). We are largely inspired by the recent rapid progress in unsupervised representation learning for photo recognition [5, 4]. However these methods are unsuited to SBIR for the key reason that they are designed for single-domain (photo) representation learning, while SBIR involves *cross-domain* data with a mixture of realistic photos and abstract/iconic sketches (Figure 1). Successful SBIR has thus far relied on sketch-photo pairings and category annotations to drive explicit sketch-photo domain alignment prior to retrieval [29, 37, 23, 22, 10]. The key question for us is how such alignment can be induced just by working with the raw unannotated and unpaired photos and sketches.

A naive solution could be unsupervised estimation of one-to-one (hard) pairings between sketch and photo for training. This will however introduce noisy labels which ultimately hinder the performance [13, 40]. Furthermore there is a chicken-and-egg problem: Any estimation of pairing is clearly dependent on the feature representation – but without good pairing supervision, the feature representation will not properly align sketches and the corresponding photos.

At a high-level our solution is based on alternating optimization between: (i) Computing a soft (many-to-many) correspondence between sketch and photo domains based

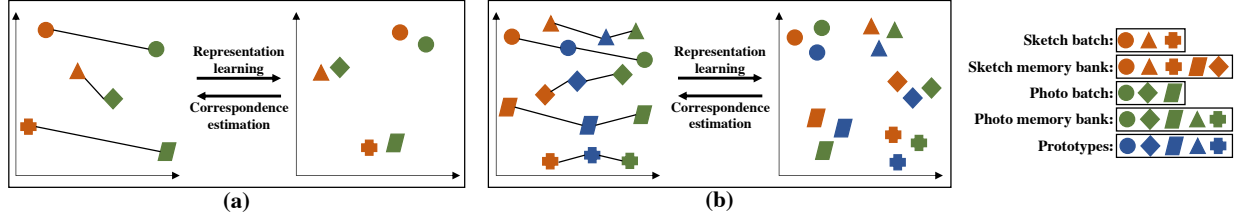


Figure 2. Comparison between batch-wise DeepJDOT [2] and our PM-JDOT. Shapes represent samples of different classes. There are five classes in total for demonstration purposes. (a) In batch-wise DeepJDOT, a single batch only contains samples from a subset of classes, so correspondence is necessarily inaccurate (mismatched shapes/categories linked) and poor alignment is learned. (b) In our PM-JDOT, (i) correspondence is mediated by learned prototypes (blue) for all classes, which enables accurate and efficient computation compactly summarizing the whole distribution; (ii) use of a memory bank allows larger sample size with more unique categories than a single batch, increasing the chance that accurate correspondence can be discovered. Note that hard pairwise correspondence is shown for ease of visualization, but actual OT correspondence computation is soft many-many.

on a distribution alignment criterion; and (ii) Learning a representation that aligns sketch and photo distributions under the soft correspondence (Figure 2). Our framework is significantly more performant and resistant to local minima compared to hard correspondence methods in other applications [13, 40] due to use of distribution alignment rather than hard pairing correspondence; and a multi-task representation learning objective that synergistically combines self-supervision and alignment objectives for semantic-aware and domain-agnostic feature learning.

In more detail, our unsupervised learning strategy starts with state-of-the-art unsupervised representation learner SwAV [4], which learns a semantically meaningful feature space by clustering and ensuring that different augmentations of the same image map to the same cluster. However, SwAV alone does not lead to representational alignment between sketch and photo domain data. To achieve this, we build on joint distribution optimal transport (JDOT) [6, 2] which learns a model together with cross-domain correspondence estimated using distribution-level information by Optimal Transport (OT) [33]. However, the original application of JDOT for multi-domain learning in CNNs [2] suffers from an inability to simultaneously provide efficiency and accuracy: OT correspondence is either inaccurate if computed at minibatch level (*e.g.*, a given sketch+photo minibatch likely contains a disjoint set of categories, and thus cannot be correctly aligned, as illustrated in Figure 2(a)); or intractable if computed at dataset level due to  $O(N^2)$  cost. We elegantly solve both of these problems by computing OT between instances and *prototypes* computed in representation learning, which provide a sparse representation of the full dataset; and extending JDOT with a feature memory bank to aggregate information across batches. We term our prototype and memory-enhanced algorithm PM-JDOT (Figure 2(b)).

Our main contributions are summarized as follows: (i) We provide the first study of unsupervised SBIR. (ii) We propose a novel unsupervised learning algorithm for multi-domain data that jointly performs alignment and solving for

latent correspondence. (iii) The cluster prototypes and feature memory banks introduced by our PM-JDOT algorithm alleviates the limits of existing JDOT, enabling effective yet tractable distribution alignment. (iv) Extensive experiments on Sketchy-Extended and TUBerlin-Extended datasets illustrate the promise of our framework in both unsupervised and zero-shot SBIR settings.

## 2. Related Work

**Sketch-based image retrieval** SBIR methods into two groups according to granularity: Category-level SBIR aims to rank photos so that those with the same semantic class as the input sketch appear first. Fine-grained SBIR targets on retrieving the specific photo corresponding to the query instance. Traditional supervised SBIR algorithms learn class-discriminative feature using classification loss [29] and remedy the domain gap with sketch-photo paired data [37, 31]. On account of the data shortage that results from labour-intensive sketch-photo paired dataset collection and annotation, zero-shot SBIR intends to test on novel categories that are unseen during training. Representative approaches use adversarial training strategy [10, 22] or triplet ranking loss [36] to learn a common feature space for both domains. Additional side information like word embeddings [9] may also be exploited to preserve semantic information. Nevertheless, annotated training data is still necessary in existing zero-shot SBIR approaches to perform effective training, and the required cross-category generalization is still an active research question [23]. We are therefore motivated to study unsupervised category-level SBIR that does not rely on sketch-photo annotations.

**Unsupervised deep learning** Unsupervised deep learning methods have recently made strong progress in representation learning that ultimately diminishes the demand for data annotation. Most contemporary unsupervised learning methods can be classified into four categories according to the learning objective: (i) Deep clustering approaches are designed to model the feature space via data grouping where the pseudo class label can be assigned either with

the help of a standard clustering algorithm [3] or by jointly learning cluster centers [14]. (ii) Instance discrimination [34] treats every single sample as a unique class, which can be beneficial to capture discriminative features of individual instance. (iii) Self-supervised learning algorithms learn through solving different pretext tasks including image colorization [39], image super-resolution [19], image in-painting [25], solving jigsaw puzzle [21], rotation prediction [15]. (iv) Contrastive learning aims to maximize agreement between different augmentations of the same input in feature space [5] or label space [4]. However, these methods are designed for single domain representation learning, and perform poorly if applied directly to multi-domain data.

A few self-supervised methods have been defined for multi-domain data [32], but these normally assume that cross-domain pairing is the ‘free’ pre-text task label, which is exactly the annotation we want to avoid. In contrast, our model performs unsupervised learning in each domain, while simultaneously aligning the domains through JDOT.

**Joint distribution optimal transport** Optimal transport [33] is a mathematical theory that enables distance measurement between distributions by way of searching for the optimal transportation plan to match samples from both distributions, and calculating the cost of that plan. Optimal transport has been applied in domain adaptation [7, 26, 35] to learn a transportation plan between source and target domains, followed by training a classifier for target domain with transported source domain data and the corresponding category annotation. To avoid this two-step process (feature transformation and classification model training), JDOT [6] aligns the feature-label joint distribution and projects input samples from both domains onto a common feature space where a classifier can be shared. DeepJDOT [2] extends JDOT to deep learning and facilitates training on large scale datasets by introducing a stochastic approximation via batch-wise optimal transport. However, we observe that data in a single batch is not informative enough to represent the whole data distribution, which limits the efficacy of optimal transport in DeepJDOT. To this end, we introduce PM-JDOT which employs cluster prototypes and feature memory banks to enhance representation of each distribution for optimizing OT-based cross-domain alignment.

### 3. Methodology

In SBIR, the goal is to train an effective CNN  $f_\theta : I \rightarrow \mathbf{x}$  to project input imagery  $I$  from both sketch and photo domains into a common embedding space, where features  $\mathbf{x}$  facilitate cross-domain instance similarity measurement. Given a query sketch  $I^s$ , a ranked list of photos will be generated according to their feature space distance to the query with the aim of ranking photos of the same category on top of the list. In the proposed unsupervised setting, we only

have access to a set of training sketches  $\mathcal{I}^s = \{I_i^s\}_{i=1}^M$  and photos  $\mathcal{I}^p = \{I_j^p\}_{j=1}^N$  that contain the same categories, but without category or sketch-photo pairing annotations – thus raising the challenge of how to learn a representation suitable for retrieval in absence of known correspondence.

To solve this problem, our method integrates two objectives: (i) unsupervised feature representation learning that encodes discriminative semantic features from visual input, and (ii) cross-domain alignment through minimizing the discrepancy between sketch and photo domain data via PM-JDOT, which employs the aggregated data in trainable cluster prototypes and feature memory banks in support of accurate and scalable discrepancy measurement. Figures 2–3 briefly summarize our unsupervised SBIR framework.

#### 3.1. Unsupervised representation learning

Our first step is to define an initial representation learning objective to learn a semantically meaningful representation (*i.e.*, ensure samples from the same domain and same category are similar in feature space) from unannotated pixel-level input images. Note that this does not yet ensure that photos and sketches from the same category are aligned, which is addressed in the following section.

We follow state-of-the-art SwAV [4], to train feature extractor  $f_\theta$  by classifying data into clusters (*i.e.*, predicting cluster assignments) and contrasting the cluster assignments for different variants of the same image. Every single sketch in  $\mathcal{I}^s$  or photo sample in  $\mathcal{I}^p$  is treated equally regardless of the corresponding source domain in this unsupervised training step. Thus later in this section, we use  $I_i$  to denote either sketch or photo instance. The training objective is to minimize the semantic representation loss:

$$\begin{aligned} L_{se} &= l(\mathbf{p}_{i^1}, \mathbf{z}_{i^2}) + l(\mathbf{p}_{i^2}, \mathbf{z}_{i^1}) \\ &= - \sum_{k=1}^K \mathbf{z}_{i^2}^{(k)} \log(\mathbf{p}_{i^1}^{(k)}) - \sum_{k=1}^K \mathbf{z}_{i^1}^{(k)} \log(\mathbf{p}_{i^2}^{(k)}) \end{aligned} \quad (1)$$

Here  $\mathbf{p}_{i^t}$  and  $\mathbf{z}_{i^t}$  are predicted cluster probability and cluster assignment of  $I_{i^t}$  respectively.  $\{\mathbf{p}_{i^1}, \mathbf{z}_{i^1}\}$  and  $\{\mathbf{p}_{i^2}, \mathbf{z}_{i^2}\}$  correspond to two transformed variants  $I_{i^1} = T_1(I_i)$  and  $I_{i^2} = T_2(I_i)$  of the same original image  $I_i$ , where  $T_1$  and  $T_2$  are randomly sampled from the set  $\mathcal{T}$  of image transformations including rescaling, flipping, *etc.*  $K$  is the cluster number. Through *swapped prediction*, *i.e.*, pairing  $\mathbf{p}_{i^1}$  with  $\mathbf{z}_{i^2}$  and  $\mathbf{p}_{i^2}$  with  $\mathbf{z}_{i^1}$  in cross-entropy loss  $l$ , the network learns to predict consistent cluster probabilities for different augmentations of identical image, which assists semantically-aware feature learning.

**Measurement for cluster probability** Cluster probability  $\mathbf{p}_{i^t}$  is calculated by introducing  $K$  trainable cluster prototypes  $\mathbf{U} = [\mathbf{u}_1, \mathbf{u}_2, \dots, \mathbf{u}_K]$  which serves as a classification layer:

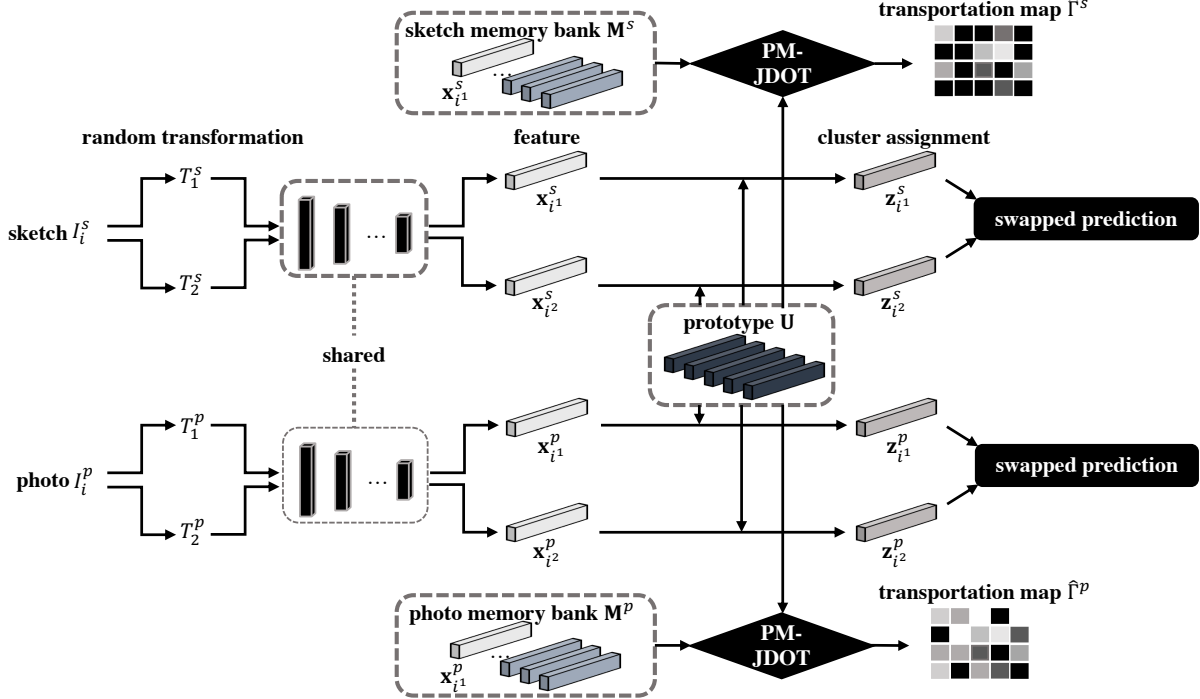


Figure 3. Schematic of our proposed framework. Sketches and photos are projected into a common feature space by unsupervised representation learning and distribution alignment.

$$\mathbf{p}_{i^t}^{(k)} = \frac{\exp(\mathbf{x}_{i^t}^\top \mathbf{u}_k / \tau)}{\sum_{j=1}^K \exp(\mathbf{x}_{i^t}^\top \mathbf{u}_j / \tau)} \quad (2)$$

where  $\mathbf{x}_{i^t} \in \mathbb{R}^D$  is the feature of  $I_{i^t}$  extracted by  $f_\theta$  and  $\tau$  is a temperature hyperparameter.

**Prediction for cluster assignment** To evaluate  $L_{se}$  (Equation 1), we also need to compute cluster assignment  $\mathbf{z}$  online at each iteration. We follow SwAV [4] and predict the cluster assignment by optimizing:

$$\max_{\mathbf{Z} \in \mathcal{Z}} \text{Tr}(\mathbf{Z}^\top \mathbf{U}^\top \mathbf{Q}) + \epsilon H(\mathbf{Z}) \quad (3)$$

$$\mathcal{Z} = \left\{ \mathbf{Z} \in \mathbb{R}_+^{K \times B} \mid \mathbf{Z} \mathbf{1}_B = \frac{1}{K} \mathbf{1}_K, \mathbf{Z}^\top \mathbf{1}_K = \frac{1}{B} \mathbf{1}_B \right\} \quad (4)$$

Where  $\mathbf{Q}$  is a feature queue of size  $B$  which is initialized with image features and updated continuously in a first-in-first-out (FIFO) manner during training. If the training batch size is  $A$ , the current batch features define the top  $A$  elements in  $\mathbf{Q}$ .  $\mathbf{Z}$  are cluster assignments corresponding to the  $B$  samples in  $\mathbf{Q}$ . Feature  $\mathbf{x}$  in  $\mathbf{Q}$  is more likely to be assigned to cluster  $k$  if  $\mathbf{u}_k$  is its nearest prototype through maximizing the similarity between the features in  $\mathbf{Q}$  and prototypes  $\mathbf{U}$  as in Equation 3.  $H(\cdot)$  is an entropy penalty with weight  $\epsilon$ . To prevent the degenerate outcome of allocating identical cluster assignment to all samples,  $\mathbf{Z}$  is subject to  $\mathcal{Z}$  to ensure the  $B$  samples in  $\mathbf{Q}$  are equally partitioned into  $K$  clusters. Feature queue  $\mathbf{Q}$ , augments the current batch with features from previous batches, to deal with

the case where the batch size  $A$  is small compared to cluster number  $K$  and cannot be equally partitioned. Only the cluster assignments for current batch, *i.e.*, top  $A$  elements in  $\mathbf{Z}$ , are required for  $L_{se}$ .

### 3.2. Cross-domain alignment

The algorithm so far in Section 3.1 learns a rich representation without external supervision, but does nothing to align the representations of semantically equivalent sketches and photos, as required for our objective of *cross-domain retrieval*. In order to support the objective of retrieving photos of the same category as a given query sketch, we introduce machinery to ensure that we learn a feature space that aligns sketch and photo distributions.

**From JDOT to PM-JDOT** We build on joint distribution optimal transport (JDOT) to align distributions from the sketch and photo domains. Crucially, we extend it to improve both alignment accuracy and efficiency by redefining the problem in terms of OT between a set of learnable prototypes and feature memory banks – PM-JDOT. Conventional JDOT aligns sets of *instances*  $\{f_\theta(I_i^s)\}_{i=1}^M$  and  $\{f_\theta(I_j^p)\}_{j=1}^N$  via computing the optimal transport plan between them and minimizing its cost. To make this quadratic computation scale to neural network training, JDOT is applied between two randomly selected batches [2]. However, an individual sketch/photo batch is a weak representation for the overall data distribution of one domain, leading to poor correspondence and hence poor cross-domain align-

ment as illustrated in Figure 2. Thus we exploit the trainable prototypes  $\mathbf{U}$  from Section 3.1 as a stronger proxy to learn a better alignment. Specifically, instead of aligning sketch and photo batches in isolation, we align both sketches and photos to our common set of prototypes which compactly represent the whole dataset by accumulating information from all training batches, into a small number of elements.

To further alleviate the limitation caused by the impoverished domain representation, *i.e.*, a small batch of samples, we introduce feature memory banks of size  $E$  for sketch  $\mathbf{M}^s = [\mathbf{x}_1^s, \mathbf{x}_2^s, \dots, \mathbf{x}_E^s]$  and photo  $\mathbf{M}^p = [\mathbf{x}_1^p, \mathbf{x}_2^p, \dots, \mathbf{x}_E^p]$  as richer domain representations for JDOT by augmenting current batch with samples in previous batches. The update strategy of memory bank is FIFO as well.

**Cross-domain mapping search** In PM-JDOT, the optimal cross-domain mapping  $\Gamma$  is found from the set of transportation plans  $\Pi$  between prototypes and one feature memory bank by minimizing:

$$\min_{\Gamma \in \Pi} \sum_{i=1}^K \sum_{j=1}^E \Gamma_{ij} \mathbf{C}(i, j) - \lambda H(\Gamma) \quad (5)$$

$$\Pi = \left\{ \Gamma \in \mathbb{R}_+^{K \times E} \mid \Gamma \mathbf{1}_E = \frac{1}{K} \mathbf{1}_K, \Gamma^\top \mathbf{1}_K = \frac{1}{E} \mathbf{1}_E \right\} \quad (6)$$

where  $H(\cdot)$  is an entropy regularization term weighted by  $\lambda$ .  $K$  and  $E$  are the number of prototypes and the size of feature memory bank respectively.  $\mathbf{C} \in \mathbb{R}^{K \times E}$  is the matrix of cross-domain pairwise costs. Specifically, the cost  $\mathbf{C}(i, j)$  of aligning  $i$ th prototype and  $j$ th element in memory bank in the joint feature-label space is calculated by:

$$\mathbf{C}(i, j) = \alpha d_f(\mathbf{u}_i, \mathbf{x}_j) + \beta d_l(\mathbf{v}_i, \mathbf{y}_j) \quad (7)$$

where cosine distance  $d_f$  is used to measure the feature-wise similarity between prototype vector  $\mathbf{u}_i$  and image feature  $\mathbf{x}_j$  extracted with  $f_\theta$ .  $d_l$  is the squared Euclidean distance applied label-wise to evaluate the difference between pre-defined one-hot label  $\mathbf{v}_i$  for  $i$ th prototype and cluster probability  $\mathbf{y}_j$  for  $j$ th image in the memory bank.  $\mathbf{v}_i$  is generated automatically according to the index  $i$  and  $\mathbf{y}_j$  is calculated by Equation 2.  $\alpha$  and  $\beta$  are scalar hyperparameters that control the contributions of feature and label distance measurements. PM-JDOT is executed twice for prototype-sketch and prototype-photo memory correspondence, producing  $\hat{\Gamma}^s$  and  $\hat{\Gamma}^p$  respectively. Feature extractor  $f_\theta$  and prototypes  $\mathbf{U}$  are fixed in this process.

**Feature extractor update** To train the feature extractor  $f_\theta$  and prototypes  $\mathbf{U}$ , we leverage the first  $A$  columns in the optimal transportation map  $\hat{\Gamma}^s$  and  $\hat{\Gamma}^p$ , which contain the mapping between trainable prototypes and current sketch/photo batch. Then the feature extractor and trainable prototypes are updated by minimizing the alignment loss between prototypes and current batch:

$$\begin{aligned} & L_a^s(\hat{\Gamma}^s) + L_a^p(\hat{\Gamma}^p) \\ &= \left( \sum_{i=1}^K \sum_{j=1}^A \hat{\Gamma}_{ij}^s (\alpha d_f(\mathbf{u}_i, \mathbf{x}_j^s) + \beta d_c(\mathbf{v}_i, \mathbf{y}_j^s)) \right) \\ &+ \left( \sum_{i=1}^K \sum_{j=1}^A \hat{\Gamma}_{ij}^p (\alpha d_f(\mathbf{u}_i, \mathbf{x}_j^p) + \beta d_c(\mathbf{v}_i, \mathbf{y}_j^p)) \right) \end{aligned} \quad (8)$$

where cross-entropy loss  $d_c$  measures label discrepancy.

**Summary** Given fixed  $f_\theta$  and  $\mathbf{U}$ , Equation 5 estimates correspondence between prototypes and images in one domain. Equation 8 provides the other part of the alternating optimization: Given a fixed set of prototype-sketch and prototype-photo correspondences, *i.e.*,  $\hat{\Gamma}^s$  and  $\hat{\Gamma}^p$ , update the  $f_\theta$  and  $\mathbf{U}$  to minimize the sum of pairwise distances. The feature extractor is trained to extract features that are domain invariant (aligned across domains), yet sensitive to semantic category. Thus, a common feature space is learned in which SBIR can ultimately be conducted directly.

### 3.3. Algorithm

The overall learning objective is to train an effective feature extractor  $f_\theta$  to capture class-discriminative yet domain-invariant features for both sketch and photo without class or instance-paired annotation. We achieve this by minimizing the semantic representation loss  $L_{se}$  (Section 3.1) and alignment loss  $L_a^s + L_a^p$  (Section 3.2) as:

$$\begin{aligned} & \text{argmin}_{\theta, \mathbf{U}} \mu L_{se} + \nu (L_a^s(\hat{\Gamma}^s) + L_a^p(\hat{\Gamma}^p)) \\ \text{s.t. } & \hat{\Gamma}^s = \arg \min_{\Gamma^s} \sum_{i=1}^K \sum_{j=1}^E \Gamma_{ij}^s \mathbf{C}^s(i, j) - \lambda H(\Gamma^s) \\ & \hat{\Gamma}^p = \arg \min_{\Gamma^p} \sum_{i=1}^K \sum_{j=1}^E \Gamma_{ij}^p \mathbf{C}^p(i, j) - \lambda H(\Gamma^p) \end{aligned} \quad (9)$$

where  $\mu$  and  $\nu$  are respective loss weights. Since the alignment loss depends on the transport plans  $\Gamma$ , we solve this by alternating optimization, as summarized in Algorithm 1.

---

#### Algorithm 1: Unsupervised SBIR training

---

##### **Input:**

Sketches  $\mathcal{I}^s$ ; Photos  $\mathcal{I}^p$ ;

##### **Output:**

Feature extractor  $f_\theta$

- 1: **repeat**
- 2:    Randomly select a mini-batch  $\{I_i^s, I_i^p\}_{i=1}^A$ ;
- 3:    Update feature queue  $\mathbf{Q}$ , sketch memory bank  $\mathbf{M}^s$  and photo memory bank  $\mathbf{M}^p$
- 4:    Fix feature extractor  $f_\theta$  and prototypes  $\mathbf{U}$ , and solve for  $\hat{\Gamma}^s$  and  $\hat{\Gamma}^p$  as in Equation 5;
- 5:    Fix  $\hat{\Gamma}^s$  and  $\hat{\Gamma}^p$ , and update feature extractor  $f_\theta$  and prototypes  $\mathbf{U}$  according to Equation 9;
- 6: **until** Convergence or max training iterations

---

Table 1. Unsupervised SBIR results on Sketchy-Extended and TUBerlin-Extended dataset

Method	Sketchy-Extended dataset			TUBerlin-Extended dataset		
	Prec@200(%)	mAP@200 (%)	mAP (%)	Prec@200(%)	mAP@200 (%)	mAP (%)
RotNet [15]	2.26	4.89	1.54	1.53	3.61	0.77
ID [34]	3.41	5.26	2.45	2.66	5.35	1.35
CDS [18]	2.37	3.58	1.88	2.64	4.69	1.63
GAN [16]	2.45	4.66	1.43	1.56	3.45	0.69
SwAV [4]	10.87	12.51	10.15	3.36	5.81	2.89
DSM [27]	10.07	17.92	4.28	7.05	13.00	2.61
SwAV [4] + CycleGAN [41]	4.15	5.39	4.28	2.67	3.50	2.06
SwAV [4] + GAN [16]	22.96	25.48	18.82	10.92	13.46	8.43
Ours	<b>33.64</b>	<b>36.31</b>	<b>28.17</b>	<b>14.78</b>	<b>18.66</b>	<b>9.93</b>

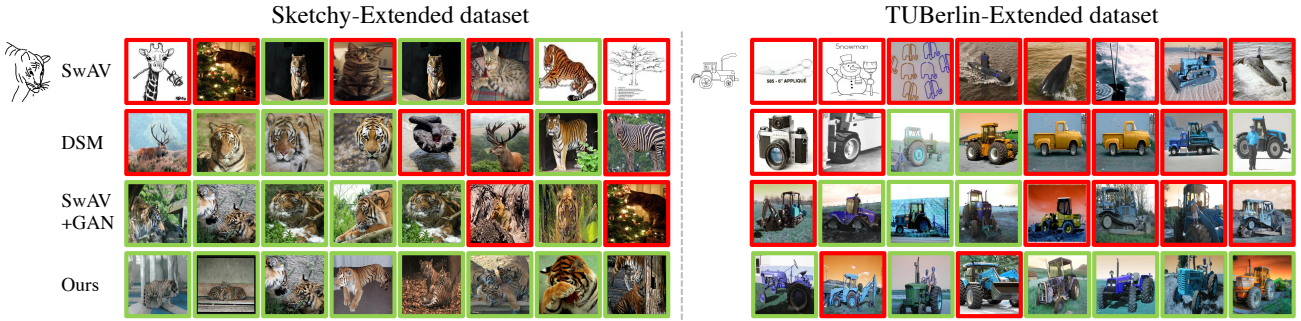


Figure 4. Top8 retrieval results for unsupervised SBIR. Row 1&amp;5: Retrieval results of SwAV [4]; Row 2&amp;6: Retrieval results of DSM [27]; Row 3&amp;7: Retrieval results of SwAV [4] + GAN [16]; Row 4&amp;8: Retrieval results of our framework.

## 4. Experiments

### 4.1. Datasets and Settings

**Datasets** We evaluate our algorithm on two datasets: (i) Sketchy-Extended [20] contains 75,471 free-hand sketches and 12,500 photos spanning over 125 categories provided by [29] and another 60,502 photos collected in [20] from ImageNet [8]. (ii) TUBerlin-Extended [38] offers 20,000 sketches [11] evenly distributed on 250 classes and photos of same categories collected using Google image search.

**Implementation details** We use ResNet-50 [17] as feature extractor  $f_\theta$ , followed by an additional L2 normalization layer to transform visual input into 128-d feature embeddings.  $f_\theta$  is first initialized with parameters pre-trained with photos in ImageNet dataset [8] by applying SwAV [4] to guarantee no labeled data is used. All training photo features extracted with the pre-trained  $f_\theta$  are grouped into  $K$  clusters using K-means. The  $K$  cluster centroids are then employed to initialize prototypes  $\mathbf{U}$ . The number of prototypes  $K$  is set to the actual number of training categories, *i.e.*, 125 for Sketchy-Extended and 250 for TUBerlin-Extended in unsupervised SBIR. The sum of elements related to current batch in  $\hat{\Gamma}^s$  and  $\hat{\Gamma}^p$  are normalized to 1 in Equation 8 for all experiments. Both the feature extractor and prototypes are trained with learning rate initialized with 0.01 and divided by 2 after each 10 epochs. Our framework is implemented with Pytorch [24] and optimal transportation plans are computed by the POT toolbox [12].

**Evaluation metrics** Cross-domain retrieval is performed

by computing cosine distance between sketch and photo feature vectors and generating a ranked list of gallery photos. We evaluate the retrieval performance by calculating the precision and mean average precision among top 200 retrieved photos denoted by Prec@200 and mAP@200 as well as the mean average precision over the whole dataset (mAP). Photos belonging to the same category as the query sketch are considered as correct retrievals.

## 4.2. Results

### 4.2.1 Unsupervised SBIR

**Settings** 50 and 10 sketches for each class are randomly selected as query sets for Sketchy-Extended and TUBerlin-Extended dataset respectively for testing. The remaining sketches and photos are used during the training process by following the same setting in [20]. No category labels or sketch-photo pairings are available during training. Each mini-batch contains 128 96  $\times$  96 pixel sketches and photos. Hyperparameters  $\alpha$ ,  $\beta$ ,  $\mu$ ,  $\nu$  are set to 0.1, 0.001, 1, 10.

**Models for comparison** We compare our method with the following unsupervised representation learning methods:

**RotNet [15]** A self-supervised method that uses rotation prediction as the pretext task. Here, we perform 4-class ( $0^\circ$ ,  $90^\circ$ ,  $180^\circ$ ,  $270^\circ$ ) classification.

**ID [34]** Instance-discrimination for unsupervised representation learning, ignoring image domain.

**CDS [18]** A self-supervised cross-domain method that carries performs intra-domain instance discrimination and cross-domain matching for representation learning.

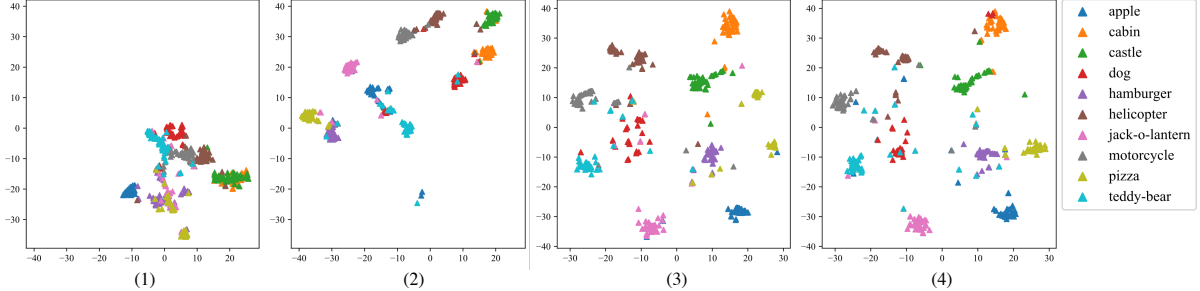


Figure 5.  $t$ -SNE visualization of 10 categories from Sketchy-Extended dataset. (1): Sketch feature visualization of SwAV [4]; (2): Photo feature visualization of SwAV [4]; (3): Sketch feature visualization of our method; (4) Photo feature visualization for our method.

Table 2. Zero-shot SBIR results on Sketchy-Extended and TUBerlin-Extended dataset.  $(*)^a$  represents for retrieval results on 25 test categories following the setting proposed in [28]. All methods except ours use instance-wise annotation in the train set.

Method	Supervision	Sketchy-Extended dataset			TUBerlin-Extended dataset		
		Prec@200(%)	mAP@200 (%)	mAP (%)	Prec@200(%)	mAP@200 (%)	mAP (%)
ZSIH [30]	✓	-	-	25.90 <sup>a</sup>	-	-	23.40
CVAE [36]	✓	33.30	22.50	19.59	0.30	0.90	0.50
SAN [22]	✓	32.20	23.60	-	21.80	14.10	-
SEM-PCYC [10]	✓	-	-	34.90 <sup>a</sup>	-	-	<b>29.70</b>
Doodle [9]	✓	37.04	<b>46.06</b>	<b>36.91</b>	12.08	15.68	10.94
Ours	✗	<b>38.44</b>	44.09	34.68	<b>28.36</b>	<b>31.53</b>	22.91

**GAN [16]** Adversarial learning is enabled by introducing a 3-layer MLP network as the discriminator to distinguish extracted features from both domains. While the feature extractor learns with the objective of removing domain-dependent feature and fooling the discriminator.

**SwAV [4]** An unsupervised feature representation learning algorithm where the cluster assignments for different variants of the same image are enforced to be consistent. During the training procedure, sketches and photos are mixed together ignoring the domain differences.

**DSM [27]** A feature extractor is trained with contrastive loss leveraging matching and non-matching training edgemap pairs. DSM results are generated by the pre-trained model from the original paper.

**SwAV [4] + CycleGAN [41]** CycleGAN, which achieves unpaired image translation, is first trained with unlabeled data to convert sketch to color photos. Both real photo data and images generated from sketch are then used in SwAV.

**SwAV [4] + GAN [16]** Different from GAN only method, feature extractor now aims at generating both semantic-aware and domain-discriminative feature by combining the swapping label prediction and adversarial learning together.

**Results** Quantitative retrieval results on Sketchy-Extended and TUBerlin-Extended are shown in Table 1. From the results, we make the following observations: (i) Unsupervised feature representation learning algorithms [15, 34, 4] originally designed for single-domain perform poorly when directly applied to cross-domain task like SBIR. SwAV [4] is the best among these three methods (ii) CDS [18] cannot cope with the large domain gap between sketch and photo and results in unsatisfactory per-

formance. (iii) From the comparison between GAN [16] and SwAV+GAN, we can see that additional guidance targeting on preserving semantic-discriminative feature is essential in category-level SBIR. (iv) CycleGAN fails to generate high-quality color images from sketch in large-scaled multi-class image translation. In contrast, it degrades the semantic information in the original sketch and leads to worse retrieval results compared with SwAV only. (v) Our proposed framework achieves the best retrieval accuracy compared with all these baseline methods trained without external labeled data. Regarding to the computation cost, the additional PM-JDOT takes around extra 0.56s/iter in training but yields large performance improvements compared with SwAV. Quantitative retrieval results and feature visualizations can be found in Figure 4 and Figure 5.

#### 4.2.2 Zero-shot SBIR

**Settings** We use the same data split as [9]: 104 and 21 categories are selected for training and testing respectively for Sketchy-Extended dataset. 30 classes are randomly chosen from TUBerlin-Extended dataset for testing and the rest are used for training. Following the default setting in [9], we set each mini-batch to 20  $224 \times 224$  sketches and photos.

**Models for comparison** Here, we compare with recent advances in zero-shot SBIR. Note that the other competitors leverage sketch-photo pairing or class label annotation to train the model while ours does not.

**ZSIH [30]** Sketch and photo are encoded into binary codes for retrieval. Sketch-photo heterogeneity is remedied by Kronecker fusion layer, graph convolution and word embeddings.

Table 3. Ablation study on our model components. Unsupervised SBIR on Sketchy-Extended and TUBerlin-Extended dataset.

Method	JDOT	Proto.	Mem. bank	Sketchy-Extended dataset			TUBerlin-Extended dataset		
				Prec@200(%)	mAP@200 (%)	mAP (%)	Prec@200(%)	mAP@200 (%)	mAP (%)
v1	$\times$	$\times$	$\times$	10.87	12.51	10.15	3.36	5.81	2.89
v2	$\checkmark$	$\times$	$\times$	21.07	23.19	18.53	7.01	9.96	5.05
v3	$\checkmark$	$\checkmark$	$\times$	25.60	28.62	20.98	9.01	12.26	5.62
v4	$\checkmark$	$\times$	$\checkmark$	24.83	27.67	20.78	11.71	15.66	7.53
v5	$\checkmark$	$\checkmark$	$\checkmark$	<b>33.64</b>	<b>36.31</b>	<b>28.17</b>	<b>14.78</b>	<b>18.66</b>	<b>9.93</b>

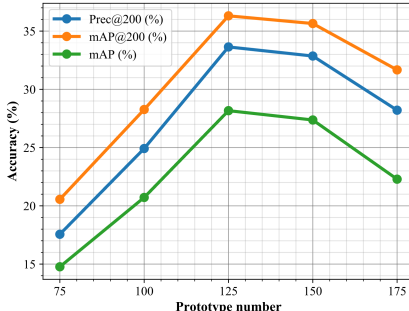


Figure 6. Prototype number  $K$  hyperparameter sensitivity. Unsupervised SBIR results on Sketchy-Extended dataset.

**CVAE** [36] Variational autoencoder is employed to model the probability distribution over images conditioned on its paired sketch feature and generate a latent prior vector. The sketch feature along with latent prior is then projected onto photo feature space.

**SAN** [22] A multi-staged generative model is designed to transform sketch feature and ensures features from different domains are encoded into a common subspace.

**SEM-PCYC** [10] Cycle-consistency is used to map data from both domains to a shared semantic space while preserving the ability to translate back to the original modality.

**Doodle** [9] Domain loss and triplet ranking loss are used to learn a common embedding space where distance between instance pairs in class-wise alignment are smaller than unaligned pairs.

**Results** Retrieval performance in Table 2 shows that even without involving human pairwise or category-level annotations during training, our framework still performs comparably with recent zero-shot SBIR algorithms that use such annotations during training. Our aligned semantically rich and domain-invariant representation learned on unlabeled training data can generalize directly to unseen classes not used for training.

#### 4.2.3 Further analysis

**Ablation Study** We analyze the efficacy of different components in our unsupervised SBIR framework in Table 3: (i) Compared with vanilla SwAV (v1), JDOT using batch-wise OT (v2) for alignment as in [2] already benefits cross-domain matching in both datasets; (ii) In v3, the transportation map is measured between prototypes and single batch of instances. The result shows that prototypes offers a

Table 4. Memory bank size hyperparameter sensitivity. Unsupervised SBIR results on Sketchy-Extended dataset.

Mem. bank size	Prec@200(%)	mAP@200 (%)	mAP (%)
no	25.60	28.62	20.98
480	27.15	30.32	22.80
960	30.36	33.54	25.59
1920	33.02	35.93	27.64
<b>3840</b>	<b>33.64</b>	<b>36.31</b>	<b>28.17</b>

better approximation for real data distribution and improves the OT-based alignment; (iii) Making use of additional data for memory bank-wise OT (v4) is also beneficial for feature alignment; and (iv) Our full model (v5), which takes advantages of both prototypes and memory banks, provides best alignment and representation learning strategy.

**Influence of prototype number** We evaluate whether the number of prototypes has an effect on the unsupervised cross-domain retrieval. The results in Figure 6 show that (i) by matching the prototype number with training category size (125 categories in Sketchy-Extended dataset), the model performs the best, so taking the class number as a known condition assists parameter optimization; (ii) slightly increasing the prototype number to 150 still leads to comparable retrieval results.

**Influence of memory bank size** To investigate the impact of our new memory bank on optimal transport-aided domain alignment, we adjust the memory bank size and show the results in Table 4. We can see that: (i) the use of memory banks indeed improves the efficacy of OT, even with a small size as 480; (ii) retrieval accuracy improves gradually with memory bank size before saturating at around size 4000.

## 5. Conclusion

This paper presents the first attempt at unsupervised SBIR, which is a more challenging learning problem, but more practically valuable due to addressing the data annotation bottleneck. To facilitate cross-domain feature representation learning with no labeled data, our proposed framework performs unsupervised representation learning and cross-domain alignment simultaneously. Alignment is further achieved accurately and scalably by our PM-JDOT. The results show that our unsupervised framework already provides usable performance on par with contemporary zero-shot SBIR methods, but without requiring any instance-wise category or pairing annotation.

## References

- [1] Ayan Kumar Bhunia, Yongxin Yang, Timothy M Hospedales, Tao Xiang, and Yi-Zhe Song. Sketch less for more: On-the-fly fine-grained sketch-based image retrieval. In *CVPR*, 2020. 1
- [2] Bharath Bhushan Damodaran, Benjamin Kellenberger, Rémi Flamary, Devis Tuia, and Nicolas Courty. Deepjdot: Deep joint distribution optimal transport for unsupervised domain adaptation. In *ECCV*, 2018. 2, 3, 4, 8
- [3] Mathilde Caron, Piotr Bojanowski, Armand Joulin, and Matthijs Douze. Deep clustering for unsupervised learning of visual features. In *ECCV*, 2018. 3
- [4] Mathilde Caron, Ishan Misra, Julien Mairal, Priya Goyal, Piotr Bojanowski, and Armand Joulin. Unsupervised learning of visual features by contrasting cluster assignments. In *NeurIPS*, 2020. 1, 2, 3, 4, 6, 7
- [5] Ting Chen, Simon Kornblith, Mohammad Norouzi, and Geoffrey Hinton. A simple framework for contrastive learning of visual representations. In *ICML*, 2020. 1, 3
- [6] Nicolas Courty, Rémi Flamary, Amaury Habrard, and Alain Rakotomamonjy. Joint distribution optimal transportation for domain adaptation. In *NeurIPS*, 2017. 2, 3
- [7] Nicolas Courty, Rémi Flamary, and Devis Tuia. Domain adaptation with regularized optimal transport. In *ECML*, 2014. 3
- [8] Jia Deng, Wei Dong, Richard Socher, Li-Jia Li, Kai Li, and Li Fei-Fei. Imagenet: A large-scale hierarchical image database. In *CVPR*, 2009. 6
- [9] Sounak Dey, Pau Riba, Anjan Dutta, Josep Llados, and Yi-Zhe Song. Doodle to search: Practical zero-shot sketch-based image retrieval. In *CVPR*, 2019. 1, 2, 7, 8
- [10] Anjan Dutta and Zeynep Akata. Semantically tied paired cycle consistency for zero-shot sketch-based image retrieval. In *CVPR*, 2019. 1, 2, 7, 8
- [11] Mathias Eitz, James Hays, and Marc Alexa. How do humans sketch objects? *ACM TOG*, 2012. 6
- [12] R’emi Flamary and Nicolas Courty. Pot python optimal transport library, 2017. 6
- [13] Yang Fu, Yunchao Wei, Guanshuo Wang, Yuqian Zhou, Honghui Shi, and Thomas S Huang. Self-similarity grouping: A simple unsupervised cross domain adaptation approach for person re-identification. In *ICCV*, 2019. 1, 2
- [14] Boyan Gao, Yongxin Yang, Henry Gouk, and Timothy M Hospedales. Deep clustering with concrete k-means. In *ICASSP*, 2020. 3
- [15] Spyros Gidaris, Praveer Singh, and Nikos Komodakis. Unsupervised representation learning by predicting image rotations. In *ICLR*, 2018. 3, 6, 7
- [16] Ian Goodfellow, Jean Pouget-Abadie, Mehdi Mirza, Bing Xu, David Warde-Farley, Sherjil Ozair, Aaron Courville, and Yoshua Bengio. Generative adversarial nets. In *NeurIPS*, 2014. 6, 7
- [17] Kaiming He, Xiangyu Zhang, Shaoqing Ren, and Jian Sun. Deep residual learning for image recognition. In *CVPR*, 2016. 6
- [18] Donghyun Kim, Kuniaki Saito, Tae-Hyun Oh, Bryan A Plummer, Stan Sclaroff, and Kate Saenko. Cross-domain self-supervised learning for domain adaptation with few source labels. *arXiv preprint arXiv:2003.08264*, 2020. 6, 7
- [19] Christian Ledig, Lucas Theis, Ferenc Huszár, Jose Caballero, Andrew Cunningham, Alejandro Acosta, Andrew Aitken, Alykhan Tejani, Johannes Totz, Zehan Wang, et al. Photo-realistic single image super-resolution using a generative adversarial network. In *CVPR*, 2017. 3
- [20] Li Liu, Fumin Shen, Yuming Shen, Xianglong Liu, and Ling Shao. Deep sketch hashing: Fast free-hand sketch-based image retrieval. In *CVPR*, 2017. 6
- [21] Mehdi Noroozi and Paolo Favaro. Unsupervised learning of visual representations by solving jigsaw puzzles. In *ECCV*, 2016. 3
- [22] Anubha Pandey, Ashish Mishra, Vinay Kumar Verma, Anurag Mittal, and Hema Murthy. Stacked adversarial network for zero-shot sketch based image retrieval. In *WACV*, 2020. 1, 2, 7, 8
- [23] Kaiyue Pang, Ke Li, Yongxin Yang, Honggang Zhang, Timothy M Hospedales, Tao Xiang, and Yi-Zhe Song. Generalising fine-grained sketch-based image retrieval. In *CVPR*, 2019. 1, 2
- [24] Adam Paszke, Sam Gross, Francisco Massa, Adam Lerer, James Bradbury, Gregory Chanan, Trevor Killeen, Zeming Lin, Natalia Gimelshein, Luca Antiga, et al. Pytorch: An imperative style, high-performance deep learning library. In *NeurIPS*, 2019. 6
- [25] Deepak Pathak, Philipp Krahenbuhl, Jeff Donahue, Trevor Darrell, and Alexei A Efros. Context encoders: Feature learning by inpainting. In *CVPR*, 2016. 3
- [26] Michaël Perrot, Nicolas Courty, Rémi Flamary, and Amaury Habrard. Mapping estimation for discrete optimal transport. In *NeurIPS*, 2016. 3
- [27] Filip Radenovic, Giorgos Tolias, and Ondrej Chum. Deep shape matching. In *ECCV*, 2018. 6, 7
- [28] Jose M Saavedra, Juan Manuel Barrios, and S Orand. Sketch based image retrieval using learned keyshapes (lks). In *BMVC*, 2015. 7
- [29] Patsorn Sangkloy, Nathan Burnell, Cusuh Ham, and James Hays. The sketchy database: learning to retrieve badly drawn bunnies. *ACM TOG*, 2016. 1, 2, 6
- [30] Yuming Shen, Li Liu, Fumin Shen, and Ling Shao. Zero-shot sketch-image hashing. In *CVPR*, 2018. 7
- [31] Jifei Song, Qian Yu, Yi-Zhe Song, Tao Xiang, and Timothy M Hospedales. Deep spatial-semantic attention for fine-grained sketch-based image retrieval. In *ICCV*, 2017. 1, 2
- [32] Yonglong Tian, Dilip Krishnan, and Phillip Isola. Contrastive multiview coding. *arXiv preprint arXiv:1906.05849*, 2019. 3
- [33] Cédric Villani. *Optimal transport: old and new.* SSBM, 2008. 2, 3
- [34] Zhirong Wu, Yuanjun Xiong, Stella X Yu, and Dahua Lin. Unsupervised feature learning via non-parametric instance discrimination. In *CVPR*, 2018. 3, 6, 7

- [35] Yuguang Yan, Wen Li, Hanrui Wu, Huaqing Min, Mingkui Tan, and Qingyao Wu. Semi-supervised optimal transport for heterogeneous domain adaptation. In *IJCAI*, 2018. [3](#)
- [36] Sasi Kiran Yelamarthi, Shiva Krishna Reddy, Ashish Mishra, and Anurag Mittal. A zero-shot framework for sketch based image retrieval. In *ECCV*, 2018. [2](#), [7](#), [8](#)
- [37] Qian Yu, Feng Liu, Yi-Zhe Song, Tao Xiang, Timothy M Hospedales, and Chen-Change Loy. Sketch me that shoe. In *CVPR*, 2016. [1](#), [2](#)
- [38] Hua Zhang, Si Liu, Changqing Zhang, Wenqi Ren, Rui Wang, and Xiaochun Cao. Sketchnet: Sketch classification with web images. In *CVPR*, 2016. [6](#)
- [39] Richard Zhang, Phillip Isola, and Alexei A Efros. Colorful image colorization. In *ECCV*, 2016. [3](#)
- [40] Xinyu Zhang, Jiewei Cao, Chunhua Shen, and Mingyu You. Self-training with progressive augmentation for unsupervised cross-domain person re-identification. In *ICCV*, 2019. [1](#), [2](#)
- [41] Jun-Yan Zhu, Taesung Park, Phillip Isola, and Alexei A Efros. Unpaired image-to-image translation using cycle-consistent adversarial networks. In *ICCV*, 2017. [6](#), [7](#)